

## Meson Form-factors and Wave-functions with Wilson fermions

Rajan Gupta, David Daniel and Jeffrey Grandy <sup>a</sup>

<sup>a</sup>T-8, MS B-285, Los Alamos National Laboratory, Los Alamos, New Mexico 87545, U. S. A.

Results for semi-leptonic form-factors for processes like  $D \rightarrow Kl\nu$  and the Bethe-Salpeter amplitudes (BSA) for pion and rho mesons are presented. The form-factor data is consistent with previous calculations. We find that the long distance fall-off of BSA for both  $\pi$  and  $\rho$  is very well fit by an exponential, but surprisingly the effective mass governing this fall-off is lighter than the pion's. Lastly, by studying the dependence of  $\rho$  polarization on separation direction we show that there is a measureable  $l = 2$  state in addition to  $l = 0$  in the BSA for the rho.

### 1. $D \rightarrow Kl\nu$ SEMI-LEPTONIC FORM-FACTOR

Form-factors for semi-leptonic decays of heavy-light pseudoscalars are expected to provide possibly the most stringent constraints on CKM angles. Over the last few years two groups have presented results for  $D \rightarrow Kl\nu$  and  $D \rightarrow K^*\nu$  decays [1] [2]. These results have large statistical errors, and, in certain instances, are in conflict. To resolve these discrepancies and to check for systematic errors, we have undertaken further studies using different methods. Here we report preliminary results for the case  $D \rightarrow Kl\nu$ .

All results presented in this talk were obtained using 35 lattices of size  $16^3 \times 40$  at  $\beta = 6.0$ . The Wilson action quark propagators were calculated on doubled lattices ( $16^3 \times 40 \rightarrow 16^3 \times 80$ ) using Wuppertal sources. The quark masses used are  $\kappa = 0.154$  and  $0.155$ , corresponding to pions of mass 700 and 560  $MeV$  respectively. (For further details see Ref. [3]). In the study of wavefunctions the convergence criteria (change per link) used for gauge fixing to either Coulomb or Landau gauge is  $10^{-6}$ . The results are preliminary and need to be confirmed on larger spatial lattices.

The matrix element of the vector current for a  $D \rightarrow K$  transition can be parameterized in terms of two form factors:

$$\begin{aligned} H_\mu &\equiv \langle K^-(p_K) | \bar{s} \gamma_\mu (1 - \gamma_5) c | D^0(p_D) \rangle \\ &= p_\mu f_+(q^2) + q_\mu f_-(q^2), \end{aligned} \quad (1)$$

where  $p = (p_D + p_K)$  and  $q = (p_D - p_K)$  is the momentum carried away by the leptons. For the vector current we use three different lattice transcriptions; the local current, 1-link extended cur-

rent and the conserved current. The non-local currents are symmetrized so that they are defined at integer values of  $t$ .

Table 1

Raw lattice data for matrix elements  $H_\mu$  with the 3 different transcriptions of the vector current.

	$\kappa_1 = 0.154$ $\kappa_2 = 0.135$	$\kappa_1 = 0.155$ $\kappa_2 = 0.135$
$\mathcal{M}\mathcal{E}^{\text{loc.}}(V_4, \vec{p} = 0)$	1.18(11)	1.19(16)
$\mathcal{M}\mathcal{E}^{\text{loc.}}(V_i, \vec{p} = 1)$	0.51(11)	0.72(25)
$\mathcal{M}\mathcal{E}^{\text{loc.}}(V_4, \vec{p} = 1)$	0.83(30)	0.84(40)
$\mathcal{M}\mathcal{E}^{\text{ext.}}(V_4, \vec{p} = 0)$	1.06(10)	1.07(15)
$\mathcal{M}\mathcal{E}^{\text{ext.}}(V_i, \vec{p} = 1)$	0.40(08)	0.55(19)
$\mathcal{M}\mathcal{E}^{\text{ext.}}(V_4, \vec{p} = 1)$	0.75(27)	0.76(36)
$\mathcal{M}\mathcal{E}^{\text{con.}}(V_4, \vec{p} = 0)$	1.08(10)	1.08(15)
$\mathcal{M}\mathcal{E}^{\text{con.}}(V_i, \vec{p} = 1)$	0.35(08)	0.46(16)
$\mathcal{M}\mathcal{E}^{\text{con.}}(V_4, \vec{p} = 1)$	0.85(29)	0.87(39)

The 3-point correlator is evaluated as follows: we start with a Wuppertal source light quark propagator and make a  $\gamma_5$  insertion at zero 3-momentum at  $t = 32$ . We use the result as a source for a second inversion with the charm quark mass fixed at  $\kappa = 0.135$ . This light-heavy propagator with a pseudoscalar insertion at  $t = 32$  is then contracted with a light quark propagator at  $t = 1$  with a  $\gamma_5$  to form the kaon. The contraction at the other end with the vector current is done at all intermediate times. The initial  $D$  meson is therefore always at rest and momentum is inserted through the vector current. We only consider the cases  $\vec{p}_K = (0, 0, 0)$  and  $(0, 0, 1)$  even though Wuppertal source quark propagators

allow coupling to kaons of all possible momenta. This is because the signal is poor for the higher momenta.

The raw lattice numbers for the three non-zero  $H_\mu$  are given in Table 1. There are two theoretical issues that need to be resolved before one can extract  $f_\pm$  from these numbers: the renormalization constant for all three currents and the normalization of the heavy  $c$  quark. These effects could be as large as 20% – 30% due to  $O(a)$  corrections. Ignoring both these issues, *i.e.* setting  $Z_V = 1.0$  and not correction for the heavy quark, our results using local and conserved current are given in Table 2. For momentum transfer  $\vec{p} = 0$  only  $f_0$  is non-zero, while for  $\vec{p} = (0, 0, 1)$  we get both  $f_\pm$ . These three results are shown in columns 2–4. Within the uncertainty of the statistical errors (20% – 40%) the two results are consistent and roughly agree with previous estimates. Clearly, to make progress it is important to improve the statistics and use a bigger lattice, and also to reduce  $O(a)$  artifacts in the normalization of the vector current and of heavy quarks.

Table 2

Form-factor data with local (upper half) and conserved vector current. Errors are  $\sim 20 - 40\%$ .

	$f_0(\vec{p} = 0)$	$f_+(\vec{p} = 1)$	$f_-(\vec{p} = 1)$
$\kappa_1 = 0.154$	0.98	0.73	-0.57
$\kappa_1 = 0.155$	1.07	0.85	-0.98
$\kappa_1 = 0.154$	0.90	0.67	-0.22
$\kappa_1 = 0.155$	0.97	0.76	-0.41

## 2. BETHE-SALPETER AMPLITUDES

The equal-time Bethe-Salpeter amplitude for the pion is defined as

$$\mathcal{A}_\pi(\vec{x}) = \langle 0 | \bar{d}(\vec{x}) \gamma_5 \mathcal{U}(\vec{0}, \vec{x}) u(\vec{0}) | \pi(\vec{p}, ) \rangle \quad (2)$$

where  $\mathcal{U}(\vec{0}, \vec{x})$  is a path-ordered product of gauge links that joins points  $\vec{x}$  and  $\vec{0}$  and makes the amplitude gauge invariant. This amplitude is given by the following ratio of 2-point correlators:

$$\frac{\langle 0 | \bar{d}(\vec{x}; t) \gamma_5 \mathcal{U}(\vec{0}, \vec{x}; t) u(\vec{0}; t) \bar{u}(\vec{y}; 0) \gamma_5 d(\vec{y}; 0) | 0 \rangle}{\langle 0 | \bar{d}(\vec{0}; t) \gamma_5 u(\vec{0}; t) \bar{u}(\vec{y}; 0) \gamma_5 d(\vec{y}; 0) | 0 \rangle} \quad (3)$$

There are two other related amplitudes that we consider; Coulomb gauge ( $\mathcal{C}_\pi$ ) and Landau gauge ( $\mathcal{L}_\pi$ ). These are obtained by transforming the quark propagators to Coulomb (Landau) gauge, and then calculating the ratio given in Eq. 3 with  $\mathcal{U} = 1$ , *i.e.* without including the links.

Chu *et al.* [4] investigated the simplest version of  $\mathcal{U}(\vec{0}, \vec{x})$ , *i.e.* the straight line path between points that lie along one of the lattice axis. Previous calculations show that  $\langle r^2 \rangle_\pi$  measured from the simplest gauge invariant BSA is smaller than that obtained in either Coulomb or Landau gauge and that these are 0.3 – 0.5 of the charge radius measured in experiments [4] [5]. (A better probe is density-density correlations as discussed in Ref. [4]). In this study we generalize  $\mathcal{U}$  to “fat” paths made up of smeared links and show that the resultant gauge invariant BSA is broader than fixed gauge amplitudes.

### 2.1. Gauge Invariant BSA with Smearing

We use the APE smearing method that was first introduced to enhance the signal in glueball calculations [6]. In this method each link in the spatial direction  $i$  is replaced by the sum

$$U_i^{(1)}(\vec{x}, \vec{x} + \hat{i}) = \mathcal{P} \left( U_i(\vec{x}, \vec{x} + \hat{i}) + \sum_{i=1}^4 \mathcal{S}_i(\vec{x}, \vec{x} + \hat{i}) \right) \quad (4)$$

where  $\mathcal{S}_i$  are the four spatial staples shared by the link  $U_i$ , and the symbol  $\mathcal{P}$  implies that the sum is projected back on to the group SU(3). One can iterate this smearing step as many times as necessary, using the effective fields at any step to produce still “fatter” fields; for example in the second smearing step the right hand side of Eq. 4 is constructed from smeared links produced in step one. We specify the smearing level by a superscript on  $\mathcal{A}$ , which will be 0 – 6 corresponding to the original links and six levels of smearing. We did not consider it appropriate to go beyond 6 levels of smearing on a lattice of size 16 with periodic boundary conditions.

There is no unique answer for the gauge-invariant BSA as different choices of  $\mathcal{U}$  yield different results. In Fig. 1 we show that  $\mathcal{A}_\pi^{(i)}(\vec{x}, t = 15)$  falls off less rapidly as the smearing level  $i$  is increased. The statistical errors are similar for smearing levels 1 – 6, and the data show a rough

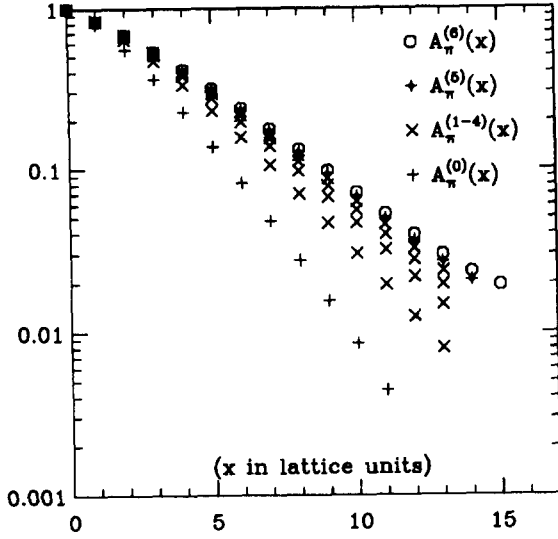


Figure 1. BSA for the pion at levels 0-6 of smearing. Errors have been suppressed for clarity

convergence with  $i$ . We therefore use results for  $i = 6$  as our present best estimate for the gauge-invariant BS amplitude. The second noteworthy feature is that the large  $x$  behavior is fit well by an exponential for  $\mathcal{A}_\pi^{(1-6)}$  for  $x \geq 6$ , while such a behavior is hard to extract from  $\mathcal{A}_\pi^{(0)}$ . We find that  $\mathcal{A}_\pi^{(6)} \sim e^{-0.3x}$ , a slower fall-off than one would expect as  $m_\pi = 0.365(6)$ . Qualitatively, the shape of the BSA does not change with  $t$ , though quantitatively it gets significantly broader with  $t$ , reaching a steady state by about  $t = 15$ . This  $t$  is somewhat larger than  $t = 10$  by which the correlator is dominated by the lightest state as shown in Ref. [3] using the same set of lattices.

We have also measured these amplitudes for non-zero momentum with the separation  $\vec{x}$  taken to be parallel or perpendicular to the direction of  $\vec{p}$ . This allowed us to qualitatively verify that the data show the expected Lorentz contraction.

## 2.2. Comparison between gauge invariant, Landau, and Coulomb gauge BSA

The Coulomb and Landau gauge amplitudes have been measured for the following relative separations: the anti-quark's position is varied in a cube of size  $9 \times 9 \times 9$  with respect to the position of the quark. For each of these relative separations

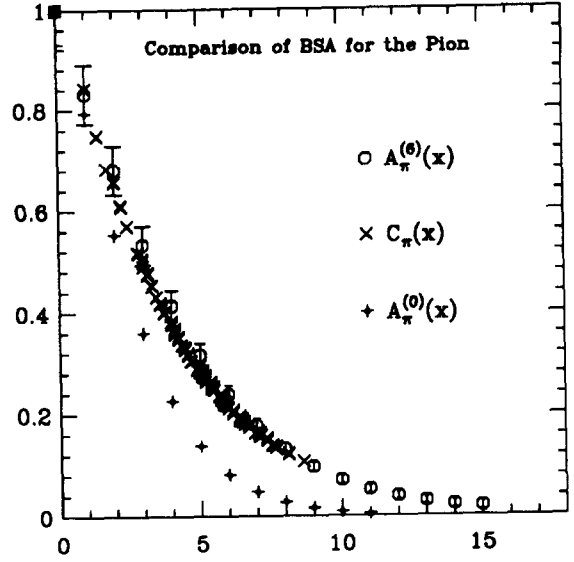


Figure 2. Comparison of the gauge-invariant BSA at smearing levels 0 and 6 with the Coulomb gauge result. We only show  $\mathcal{C}_\pi$  for  $x_i \leq 6$ .

we sum the quark's position over the time slice to produce a zero-momentum state. The data show that for  $x > 6$  along any of the axis there is a significant contamination from wrap-around effects due to periodic boundary conditions. These effects can be taken into account by incorporating the contributions of all the mirror points.

The data show that  $\mathcal{A}^{(6)}$  is slightly broader than  $\mathcal{L}$  which in turn is slightly broader than  $\mathcal{C}$ . On the other hand we find  $\mathcal{L} \gtrsim \mathcal{C} > \mathcal{A}^{(0)}$  consistent with the earlier results of Ref. [5]. These two features are illustrated in Fig. 2 by data for  $\mathcal{C}_\pi$ ,  $\mathcal{A}_\pi^{(0)}$  and  $\mathcal{A}_\pi^{(6)}$ . Thus  $\mathcal{A}^{(6)}$  is a better probe of quark/anti-quark distribution than Coulomb or Landau gauge BSA.

## 2.3. Polarization dependence of the $\rho$ BSA

The  $\rho$  meson wavefunction is a linear combination of  $l = 0$  and  $l = 2$  orbital angular momentum states. On the lattice the BSA can be decomposed under the cubic group as

$$\begin{aligned} & \langle 0 | \bar{d}(\vec{x}, t) \gamma_i \mathcal{U}(\vec{0}, \vec{x}; t) u(\vec{0}, t) | \rho(\vec{0}, j) \rangle \\ &= \frac{m_\rho^2}{f_\rho} \left[ \delta_{ij} \phi_{A_1}(\vec{x}) + \delta_{ij} \left( \frac{x_i^2}{\vec{x}^2} - \frac{1}{3} \right) \phi_E(\vec{x}) \right] \end{aligned}$$

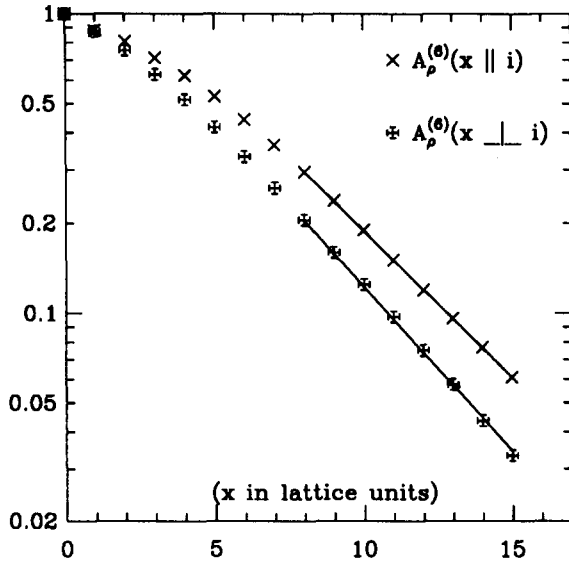


Figure 3. The BSA for the rho at  $\kappa = 0.154$  with polarization axis  $i \parallel$  and  $\perp$  to separation  $\vec{x}$ .

$$+(1 - \delta_{ij}) \frac{x_i x_j}{\vec{x}^2} \phi_{T_2}(\vec{x}) \Big]. \quad (5)$$

The functions  $\phi_{A_1}$ ,  $\phi_E$  and  $\phi_{T_2}$  are scalars under the cubic group with  $E$  ( $T_2$ ) labelling the 2 (3) dimensional decomposition of the  $l = 2$  state. Thus lattice calculations allow us to investigate, as a function of the quark mass, the relative mixture of  $l = 0$  and  $l = 2$  states, and the restoration of rotational symmetry by studying the three cases: (A)  $i = j$  and  $\vec{x}$  along  $i$  ( $\parallel$ ), (B)  $i = j$  and  $\vec{x}$  perpendicular to  $i$  ( $\perp$ ), and (C)  $i \neq j$ .

At present we have only measured the BSA for  $i = j$ , and the results for cases (A) and (B) at  $\kappa = 0.154$  are shown in Fig. 3. The data show that for large separation the fall-off is extremely well fit by an exponential in both cases, with a rate of fall-off given by  $m_{\parallel} = 0.226(8)$  and  $m_{\perp} = 0.263(7)$  respectively. Again, it is interesting to note that the large  $x$  fall-off is governed by a mass that is lighter than  $m_{\pi} = 0.365$ .

From the data shown in Fig. 3 we extract  $\phi_{A_1}(x)$  and  $\phi_E(x)$ . The results, shown in Fig. 4, are fit to simple hydrogen-like radial wavefunctions

$$\begin{aligned} \phi_{A_1}(x) &= 1.61 e^{-0.242r} \\ \phi_E(x) &= 0.029 r^2 e^{-0.375r} . \end{aligned} \quad (6)$$

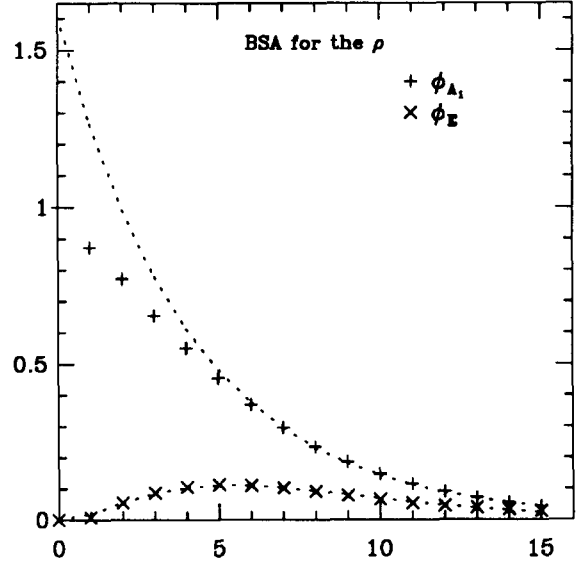


Figure 4. Results for  $\phi_{A_1}(x)$  and  $\phi_E(x)$  using the data shown in Fig. 3. The fits are described in Eq. (6).

These functions give a good fit to  $\phi_{A_1}(x)$  for  $r \geq 6$  and  $\phi_E(x)$  for  $r \geq 2$ . The results at  $\kappa = 0.155$  are qualitatively similar. The data for both  $\phi_{A_1}(x)$  and  $\phi_E(x)$  are slightly broader, though the difference is smaller than the statistical errors.

**ACKNOWLEDGEMENTS:** These calculations were done on Cray YMP using time provided by LANL, NERSC, PSC and SDSC Supercomputer centers. We thank DOE, NSF and Cray Research for their support.

## REFERENCES

- 1 C. Bernard, A. El-Khadra and A. Soni, *Phys. Rev.* **D46** (1992) 869.
- 2 V. Lubicz, G. Martinelli, M. McCarthy and C. Sachrajda, *Phys. Lett.* **274B** (1992) 415.
- 3 D. Daniel, R. Gupta, G. Kilcup, A. Patel, S. Sharpe, *Phys. Rev.* **D46** (1992) 3003.
- 4 M-C. Chu, M. Lissia and J. Negele, *Nucl. Phys.* **B360** (1991) 31.
- 5 M. Hecht and T. DeGrand, *Phys. Rev.* **D46** (1992) 2155.
- 6 APE Collab., *Phys. Lett.* **192B** (1987) 163.